

Temperature-Responsive Poly(*N*-isopropylacrylamide) Modified Gold Nanoparticle–Protein Conjugates for Bioactivity Modulation

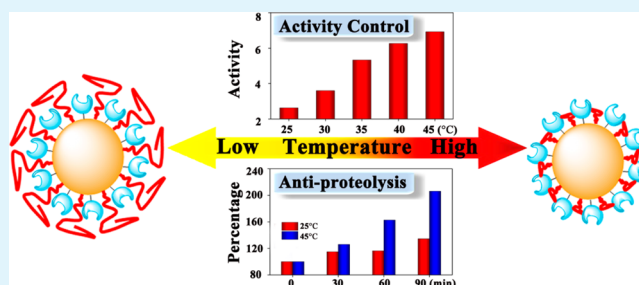
Feng Liu,[†] Yuecheng Cui,[†] Lei Wang, Hongwei Wang,* Yuqi Yuan, Jingjing Pan, Hong Chen, and Lin Yuan*

The Key Lab of Health Chemistry and Molecular Diagnosis of Suzhou, Department of Polymer Science and Engineering, College of Chemistry, Chemical Engineering and Materials Science, Soochow University, Suzhou 215123, P. R. China

S Supporting Information

ABSTRACT: It is important to effectively maintain and modulate the bioactivity of protein-nanoparticle conjugates for their further and intensive applications. The strategies of controlling protein activity via “tailor-made surfaces” still have some limitations, such as the difficulties in further modulation of the bioactivity and the proteolysis by some proteases. Thus, it is essential to establish a responsive protein-nanoparticle conjugate system to realize not only controllable modulations of protein activity in the conjugates by incorporating sensitivity to environmental cues but also high resistance to proteases. In the work reported here, *Escherichia coli* (*E. coli*) inorganic pyrophosphatase (PPase) and poly(*N*-isopropylacrylamide) (pNIPAM) were both fabricated onto gold nanoparticles (AuNPs), forming AuNP-PPase-pNIPAM conjugates. The bioactivity-modulating capability of the conjugates with changes in temperature was systematically investigated by varying the molecular weight of pNIPAM, the PPase/pNIPAM molar ratio on AuNP, and the orientation of the proteins. Under proper conditions, the activity of the conjugate at 45 °C was approximately 270% of that at 25 °C. In the presence of trypsin digestion, much less conjugate activity than protein activity was lost. These findings indicate that the fabrication of AuNP-protein-pNIPAM conjugates can both modulate protein activity on a large scale and show much higher resistance to protease digestion, exhibiting great potential in targeted delivery, controllable biocatalysis, and molecular/cellular recognition.

KEYWORDS: poly(*N*-isopropylacrylamide), protein activity, gold nanoparticle, inorganic pyrophosphatase, thermoresponsive



1. INTRODUCTION

Conjugation of proteins to nanoparticles allows for the stabilization of nanoparticles and enables the introduction of biologically active functionalities on nanomaterials.¹ Protein-nanoparticle conjugates possess great potential in many areas of bionanotechnology, including biocatalysis, drug delivery, biosensors, and bioimaging.^{2–6} In the protein–nanoparticle conjugate system, gold nanoparticles (AuNPs) are one of the most commonly utilized nanomaterials for protein conjugation due to their large surface-to-volume ratio, easily modified surface, good biocompatibility, and high protein loading.⁷

The effectiveness of the conjugates depends on the activity of the conjugated protein.⁸ However, when a protein is conjugated to a AuNP by either covalent interaction or nonspecific binding, it undergoes some loss of activity in most cases.⁹ Thus, to effectively maintain and modulate the bioactivity of the proteins in the conjugates is important for their biomedical applications. Factors that affect protein activity in the conjugates are various and complex, including the orientation and surface density of proteins on AuNPs and the surface curvature of the nanoparticles.^{10,11} Protein activity can be modulated by changing these factors. Protein orientation directly affects the entrance to the substrate channel or

interferes with the diffusion of substrates to the active site, leading to more or less loss of activity.^{12,13} Protein surface density affects lateral protein–protein interactions, steric hindrance, and the conformational structure of proteins, thereby modulating protein activity,^{14,15} and the surface curvature directly affects the conformational structure of proteins to modulate their activity.^{16,17} Many strategies for modulation of protein activity have been proposed, based on changing the above factors.⁹ Although all the reported strategies can modulate protein activity to some extent, there still exist some limitations. First, in these strategies, protein–nanoparticle conjugates are fabricated by “tailor-made surfaces.”¹⁶ Once protein–nanoparticle conjugates are prepared, the bioactivity of protein in the conjugates is difficult to further modulate. Second, proteins located on the outside of the conjugates are mostly exposed to the environment, leading to easy proteolysis by proteases. Therefore, it is essential to establish a new protein–nanoparticle conjugate system to realize not only controllable modulation of protein activity in the conjugates, by

Received: March 21, 2015

Accepted: May 7, 2015

Published: May 7, 2015

incorporating sensitivity to environmental cues, but also higher resistance of proteins to negative factors in the physiological environment, such as proteases.

Stimuli-responsive nanoparticle systems can incorporate sensitivity to a variety of environmental factors (such as temperature, pH and light).^{18–20} pNIPAM has been commonly used as a temperature-responsive material in many fields due to its ability to undergo a reversible lower critical solution temperature (LCST) phase transition from a swollen, hydrated state to a shrunken, hydrophobic state.^{21,22} pNIPAM and its derivatives have been increasingly used in fabrication of bionanomaterials.^{23,24} Mirkin's group reported DNA and pNIPAM coassembled onto AuNPs.²⁵ The DNA sequences could be reversibly hidden or exposed from the polymer surface in response to temperature changes, thereby translating the temperature trigger to the "on–off switching" of the surface chemistry and function. Salmaso's group reported that thiolated folic acid and pNIPAM were cobound on AuNPs when they used a thermoresponsive polymer to mask and display bioactive ligands for selective tumor cell targeting.²⁶

Proteins are biomolecules with the most complex functions and provide the ultimate complexity in three-dimensional structures at the nanoscale. They can have well-defined recognition properties for a wide range of molecules including small molecules, DNA, peptides, and other proteins, and operate as enzymes on substrates.¹⁸ Thus, AuNP–protein–pNIPAM conjugates are considered to have great potential in many fields. On one hand, the conjugated proteins can be sterically shielded by hydrated pNIPAM chains and be undisturbed below the LCST; on the other hand, above the LCST, the collapses of pNIPAM chains lead to the gradual exposure of protein active sites on the surface and thus the modulation of protein activity.

In the present work, AuNPs modified with pNIPAM and PPase were fabricated to demonstrate thermally responsive controllable modulation of protein activity. The bioactivity-modulating capability of the conjugates as temperature changed was systematically investigated by varying the molecular weight of pNIPAM, the PPase/pNIPAM molar ratio on AuNP, and the orientation of proteins.

2. MATERIALS AND METHODS

N-Isopropylacrylamide (NIPAM, Acros, 99%) was recrystallized from a toluene/hexane solution (50%, v/v) and dried under vacuum prior to use. 2,2'-Azobisisobutyronitrile (AIBN) from Shanghai Qiangshun Chemical Reagent Co. was recrystallized from ethanol solution and dried under vacuum prior to use. *N*-Hydroxysulfosuccinimide sodium salt and *N*-(3-(dimethylamino)propyl)-*N'*-ethylcarbodiimide hydrochloride were purchased from Aladdin Industrial Co. (Shanghai, China). Hydrogen tetrachloroaurate hydrate (HAuCl₄·4H₂O) was purchased from Sinopharm Chemical Reagent Co. (Shanghai, China). Sodium citrate tribasic dehydrates and fluoresceinamine were supplied by Sigma-Aldrich Co. (USA). DNA polymerase (PrimeStar HS), restriction endonucleases, and T₄ DNA ligase were purchased from Takara Biotechnology Co. Oligonucleotides used as the PCR primers were synthesized at Sangon Biotech (Shanghai) Co., Ltd. *p*-Chloromercuribenzoate and cysteine were purchased from Sangon Biotech (Shanghai) Co. All aqueous solutions were prepared in 18.2 MΩ·cm purified water from a Milli-Q water purification system (Millipore, Bedford, MA, USA).

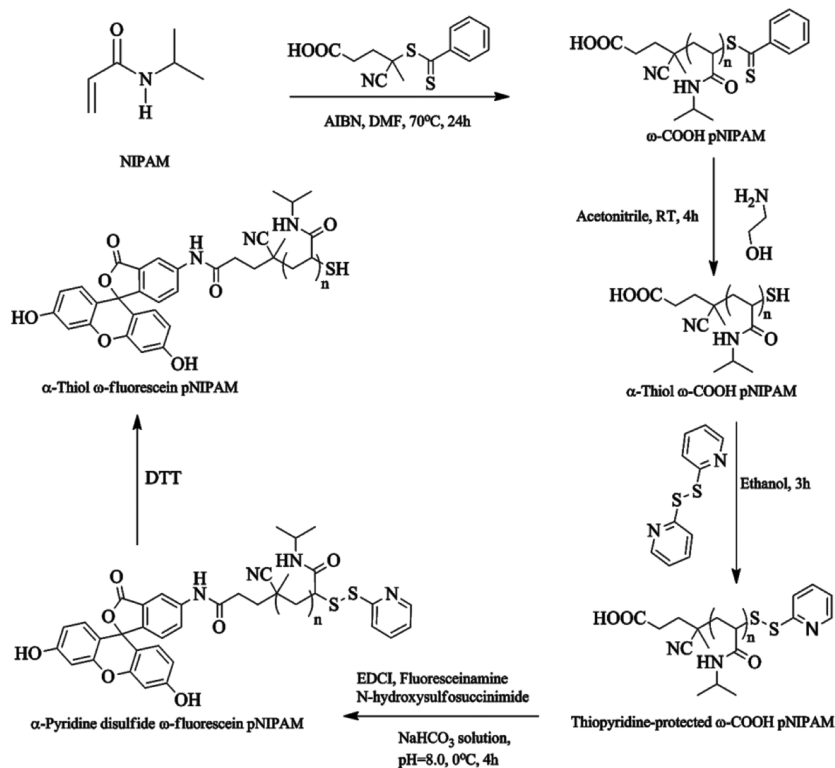
Generation of Mutant-Type PPase. Mutant-type PPases (OB1 and OB2) were generated as previously described.²⁷ Briefly, site-specific mutants were performed for cloning the mutant *ppa* gene according to the megaprimer PCR method.²⁸ The forward flanking primer sequence used in the megaprimer PCR was 5'-

CGCAAGCTTTTATTTATTTCTTTGCGCGCTC-3', and the reverse flanking primer sequence was 5'-CGCGGATCCAGCTTACTCAACGTCCCT-3'. The primer for OB1 used to create the K148C-PPase was 5'- CCTCGAAAAAGGCTGCTGGGTGAAAGTTGAAGG-3'. The primer for OB2 used to create the N124C-PPase was 5'- CACATTAAAGACGTTTGGCATCTGCCTGAACTGC-3' (nucleotides that represent mutations are underlined). The megaprimer PCR products were digested with *Bam*HI and *Hind*III and then ligated to the *Bam*HI–*Hind*III site of the pQE30 vector. The plasmids were transformed into *E. coli* XL1-Blue for protein expression. The *E. coli* XL1-Blue cells expressing the mutants and the wild-type PPase (RB) were cultured in liquid LB medium for further IPTG incubation. The cells were pelleted by centrifugation, and then the obtained cell precipitates were disrupted with lysozyme and sonicated to obtain supernatants for further purification by Ni-NTA Sepharose resin (Shanghai Sangon Biotech Co., Ltd., China). The mutants were then purified and concentrated using centrifuge filters (Amicon Ultra). The purity of the proteins was verified by sodium dodecyl sulfate-polyacrylamide gel electrophoresis (SDS-PAGE, 4% stacking gel, 12% separating gel).

Preparation of Citrate-Protected AuNPs. The citrate-protected AuNPs were prepared as the reported procedure.²⁹ In a 250 mL round-bottom flask equipped with a condenser, double-distilled water (100 mL) and HAuCl₄ (12 mM, 516 μL) were added. After the solution reached boiling temperature, sodium citrate (10% w/v, 4.4 mL) was added rapidly with vigorous stirring, resulting in the color changing from pale yellow to burgundy. Boiling was continued for another 10 min, and stirring was continued until the mixture cooled to room temperature. It should be noted that all glassware used for the preparation of AuNPs was cleaned with aqua regia solution (HCl/HNO₃ = 3:1, v/v) and rinsed thoroughly with double-distilled water prior to use.

Synthesis of α-Thiol pNIPAM. The pNIPAM was prepared via reversible addition–fragmentation chain transfer (RAFT) polymerization using 4-cyano-4-(phenylcarbonothioylthio) pentanoic acid (CTP) as the chain transfer agent (CTA) as described.²⁸ First, 1.13 g of NIPAM purified by *n*-hexane, mixed with 28 mg of CTP and 3.3 mg of AIBN, was dissolved in 5 mL of DMF in a glass round-bottom flask. The solution was purified by nitrogen for 30 min and then transferred into a glovebox. The reaction was carried out at 60 °C for 24 h. The polymer was purified using dialysis tubing (molecular weight cutoff (MWCO) = 3.5 kDa) and dialyzed for 12 h against water. The purified polymer was then lyophilized. Next, 0.1 g of pNIPAM (*M_w* = 10 000 g/mol by GPC, PDI = 1.17) was dissolved in 2 mL of acetonitrile in a glass round-bottom flask. Then, 0.1 mL of ethanolamine was added dropwise into the solution under stirring. The reaction was carried out for 4 h, and the mixture was dialyzed against water for 12 h and then lyophilized. The polymer was analyzed by DMF GPC and NMR in deuterioxide.

Synthesis of α-Thiol ω-Fluorescein pNIPAM. The pNIPAM was first modified to be thiopyridine-protected pNIPAM as reported.²⁵ Seventy-five milligrams of pNIPAM with thiol group (*M_w* = 10 000 g/mol, PDI = 1.17) and 16.52 mg of 2,2'-dithiodipyridine were dissolved in 4 mL ethanol. After stirring for 3 h, the solution was transferred to presoaked dialysis tubing (MWCO = 3.5 kDa) and dialyzed overnight against 80% ethanol/water (v/v), and then against double-deionized water for another 24 h. The polymer was lyophilized. Fifteen milligrams of thiopyridine-protected ω-COOH pNIPAM (*M_w* = 10000 g/mol by GPC, PDI = 1.17) was dissolved in 5 mL of double deionized water, mixed with 1-ethyl-3-(3-(dimethylamino)propyl) carbodiimide (EDCI, 0.1 M), *N*-hydroxysulfosuccinimide sodium salt (20 mM) and 6.5 mg of fluoresceinamine. Then, the pH of the solution was adjusted to 8.0 using aliquots of 5 μL of saturated sodium bicarbonate solution. The reaction was carried out at 0 °C for 4 h with stirring. The polymer was then dialyzed (MWCO = 3.5 kDa) against 300 mM NaCl solution for 24 h and for another 2 days against PBS (pH 7.4). The polymer was lyophilized overnight. Then, 5 mg of α-thiol ω-fluorescein pNIPAM was treated with 250 μL of 100 mM dithiothreitol (DTT) in 50 mM pH 8.0 phosphate buffer for 1 h.

Scheme 1. Synthesis of α -Thiol ω -Fluorescein pNIPAM

Thereafter, the polymer was dialyzed (MWCO = 3.5 kDa) against double-deionized water for 15 min and then lyophilized overnight.

Conjugation of PPase (RB, OB1, and OB2) and pNIPAM onto the AuNPs. The solution of prepared AuNPs was added to 500 μ L of PPase (RB, OB1 and OB2) in double-distilled water and incubated for 12 h at room temperature, ensuring that CPPase = 0.02 mM and CPPase/CAuNPs = 60/1–340/1. In order to protect the activity of PPase from pollution, the Eppendorf (EP) tubes used in the experiments must be sterilized and the conjugation must be conducted in a sterile environment. The pNIPAM was added in the mixture and incubated for another 24 h, ensuring that CpNIPAM/CAuNPs = 200/1. For removal of excess PPase and pNIPAM, PPase and pNIPAM-coated AuNPs were centrifuged at 12 000 g on an Eppendorf centrifuge 5810R for 25 min and rinsed four times. The AuNP-PPase-pNIPAM conjugates were separated from supernatant and redissolved in 500 μ L of double distilled water.

Characterization of AuNP-PPase-pNIPAM Conjugates. The surface morphology of AuNPs and AuNP-PPase-pNIPAM conjugates was investigated by transmission electron microscopy (TEM) (G-200, Hitachi, Tokyo, Japan). Size analysis was performed by dynamic light scattering (DLS) using a Zetasizer Nano-ZS90 zeta potential analyzer (Malvern Instrument Ltd. UK) at 25 and 45 $^{\circ}$ C. AuNP-PPase-pNIPAM binding was analyzed by spectrophotometry (Varioskan Flash, Thermo Scientific, USA).

PPase Activity Assay. The activity of the PPase and AuNP-PPase-pNIPAM was assayed as described.³⁰ Enzymatic hydrolysis was performed at 25 and 45 $^{\circ}$ C for 10 min in 50 mM Tris-HCl buffer (pH 8.0) including 5 μ g/mL PPase, 50 mM $MgCl_2$, and 2 mM PPI. The reaction ($V_{Total} = 100 \mu$ L) was terminated by the addition of 10 μ L 0.4 M citric acid. Then, 800 μ L AAM solution (acetone, 2.5 M sulfuric acid and 10 mM ammonium molybdate in 2:1:1 volume proportion) was added to the tubes. The contents were mixed, and then 80 μ L 1 M citric acid was added. The color change of the mixed solution was measured with a spectrophotometer at 355 nm. The protein concentration was measured by the Bradford method³¹ with bovine serum albumin (BSA) as the protein standard. The activity of native PPase (control) was taken to be 100%. From this value, the relative activity of AuNP-PPase-pNIPAM conjugates was calculated.

Quantifying PPase/pNIPAM Molar Ratio. AuNPs were first bound to PPase and then to fluorescein-pNIPAM, which is identical to that of nonfluorescein-pNIPAM AuNPs. After centrifuging and rinsing four times, the supernatant containing excessive PPase and fluorescein-pNIPAM was collected and analyzed by visible and fluorescence spectroscopy. Optical absorbance at 595 nm was measured, and the values were compared to a standard curve of known BSA concentrations, from which the amount of excessive PPase in the supernatant was calculated. Similarly, the fluorescence of the supernatant was determined (excitation, 321 nm; emission, 523 nm) and compared to a standard curve of known fluorescein-pNIPAM concentrations. Assuming that PPase and fluorescein-pNIPAM were either free in solution or bound to the AuNP surface, the amount of PPase and pNIPAM bound on AuNPs was calculated by subtracting the excessive PPase and fluorescein-pNIPAM from the known feed amount.²⁵

Stability to Trypsin Digestion of the Native PPase and the Conjugates. To measure the stability of proteins to proteolysis, samples of native PPase and the conjugates (0.01 mM) were incubated in with trypsin in 0.1 M phosphate buffer (pH 7.4) at 25 and 45 $^{\circ}$ C (molar ratio of sample/trypsin = 10/1). Aliquots were taken at various time intervals and assayed for enzymatic activity as above.

3. RESULTS AND DISCUSSION

Synthesis of α -Thiol ω -Fluorescein pNIPAM. To prepare AuNP-PPase-pNIPAM conjugates, thiol-terminated pNIPAM was first synthesized by RAFT polymerization. ω -COOH pNIPAM was polymerized by NIPAM with CPTP using AIBN as an initiator (Scheme 1). The M_w of ω -COOH pNIPAM were calculated to be 5 kDa, 10 kDa, 20 kDa and 40 kDa (Table S1 in the Supporting Information), respectively. To prepare thiol-terminated pNIPAM (α -thiol pNIPAM), the thiolester was reduced to a thiol group with ethanol amine via an aminolysis reaction. The degree of thiol modification was almost 100%, as determined from NMR (Figure S1 in the Supporting Information). The α -thiol ω -COOH pNIPAM was

protected using 2,2'-dithiodipyridine at the α -thiol position. The α -pyridine disulfide ω -fluorescein pNIPAM was prepared by conjugating pNIPAM-COOH and fluoresceinamine via NHS chemistry and carbodiimide chemistry, which was reduced by DTT to prepare the α -thiol ω -fluorescein pNIPAM.

Characterization of the AuNP-PPase-pNIPAM Conjugates. AuNP-PPase conjugates were prepared with the feed molar ratio of PPase: AuNP of 100:1, resulting in the immobilized amount of PPase per AuNP about 58. Since PPase bound with AuNPs randomly via Au-S bond at the above ratio, there remained much free space on the surface of the conjugates,³² which allowed further modifications of polymers. The final AuNP-PPase-pNIPAM conjugates were achieved by introducing pNIPAM onto the AuNP-PPase conjugates by Au-S bond. The binding of PPase and pNIPAM to AuNPs induced apparent changes in the absorption spectra of AuNPs (Figure 1). The maximum absorption peak of

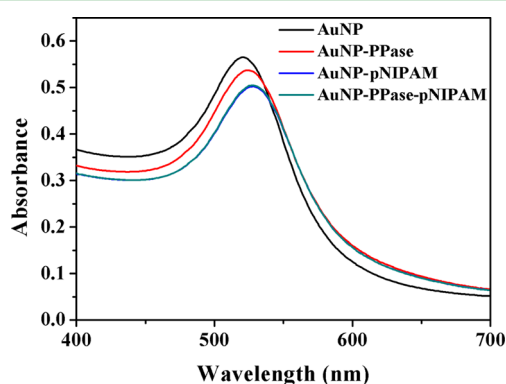


Figure 1. Characterization of AuNP-PPase-pNIPAM conjugates. Visible absorption spectra in aqueous suspension.

unmodified AuNPs was located at 521 nm; after binding of PPase, the maximum absorption peak red-shifted to 524 nm; after further binding of pNIPAM, the maximum absorption peak showed a further redshift to 528 nm, which is the maximum absorption peak of AuNP-pNIPAM.

The hydrodynamic diameters of AuNPs changed markedly after conjugation with PPase and pNIPAM. The hydrodynamic diameter of AuNPs in aqueous solution was 13.1 ± 1.5 nm; after conjugation with PPase, it increased to 15.5 ± 2.1 nm; after further conjugation with pNIPAM, the diameter of the conjugates increased to 24.1 ± 2.8 nm (at 25 °C), similar to that of AuNP-pNIPAM (27.1 ± 2.5 nm, Figure 2). The changes in morphology and size of the particles were also investigated by TEM. The AuNPs were well-dispersed (Figure S2A in the Supporting Information) and smoothly spherical with narrow hydrodynamic diameter distribution (Figure S2B in the Supporting Information). After conjugated with PPase and pNIPAM, PPase, and pNIPAM were uniformly attached on the surface of the AuNPs, indicating the formation of AuNP-PPase-pNIPAM conjugates (Figure S2B in the Supporting Information).

The hydrodynamic diameters of AuNP-PPase-pNIPAM and AuNP-pNIPAM were compared further at 25 and 45 °C. The results showed that with the temperature rising from 25 to 45 °C, the diameter of AuNP-PPase-pNIPAM decreased from 24.1 ± 1.9 to 18.1 ± 2.1 nm. The diameter change tendency of AuNP-PPase-pNIPAM conjugates was almost same as that of AuNP-pNIPAM conjugates (Figure 2). These results demon-

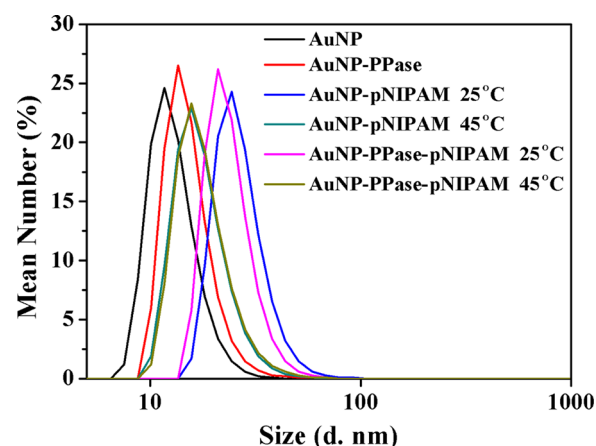


Figure 2. Characterization of AuNP-PPase-pNIPAM conjugates. Hydrodynamic diameters determined by DLS.

strate that AuNP-PPase-pNIPAM conjugates have thermosensitivity, and it would be possible to regulate protein activity by temperature change by modulating the elongated and hydrophilic state or dehydrated and collapsed state of pNIPAM chains.

Temperature-Dependent Activity of the AuNP-PPase-pNIPAM Conjugates. To investigate whether the introduction of pNIPAM onto the AuNP-PPase conjugates could regulate protein activity to a large extent, the activities of the conjugates were detected at different temperatures. The Au-S bond becomes unstable at temperature above 60 °C.³³ In the following experiments, measurements were performed at 25 to 60 °C, which is the appropriate temperature range for living organisms.³⁴ Under the testing condition in the present work, the specific activity of native PPase was 5.66 ± 0.27 kat/kg at 25 °C. As temperature increased, the activity increased gradually from 25 to 45 °C and then gradually decreased afterward, with the maximum of 7.67 ± 0.28 kat/kg at 45 °C. For the AuNP-PPase-pNIPAM conjugates, the activity increased gradually as the temperature rose from 25 to 50 °C, reaching the maximum of 7.25 ± 0.24 kat/kg at 50 °C, which was 280% of that at 25 °C (2.63 ± 0.13 kat/kg). As temperature rose above 60 °C, the activity of conjugates decreased gradually but remained higher than that of the native PPase at the same temperature (Figure 3A). Compared with native PPase, as temperature increased from 25 to 60 °C, the relative activity of the conjugates increased from $46.4 \pm 2.3\%$ at 25 °C to $90.4 \pm 3.1\%$ at 45 °C, reaching a maximum at 55 °C (approximately 110%, Figure 3B).

For native PPase, when the temperature increased from 25 to 45 °C, diffusion of substrates to active sites of the enzyme became faster, leading to increased protein activity. But a further increase in temperature would cause conformational changes of proteins and even irreversible denaturation, resulting in loss of activity.³⁵ However, the AuNP-PPase-pNIPAM conjugates exhibited thermosensitivity due to pNIPAM chains. When the environmental temperature dropped below the LCST (approximately 32 °C), the elongated and hydrophilic-state pNIPAM chains could sterically shield and cover the active sites of PPase, resulting in decreased catalytic activity; when it was above the LCST, the dehydrated and collapsed state of pNIPAM chains could expose the proteins and their active sites, resulting in the gradient increase of protein activity with the temperature increase. Such effect indicated that the

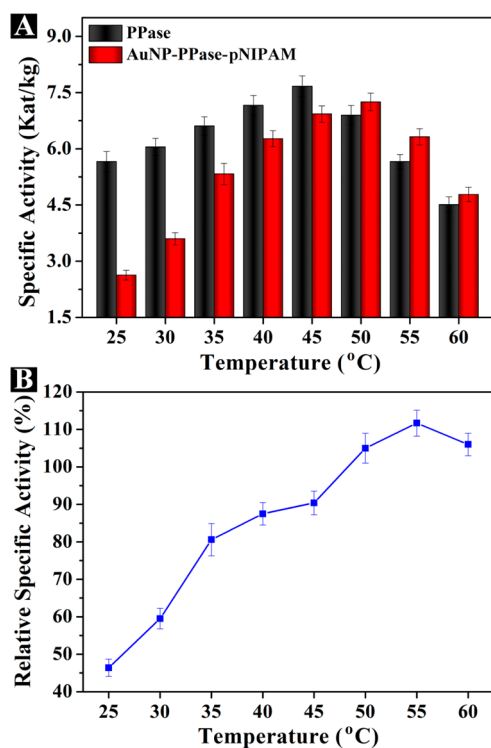


Figure 3. Temperature-dependent activity of the conjugates. (A) Specific activity of native PPase and the conjugates at different temperatures (\pm SD, $n = 3$); (B) relative specific activity of the conjugates (compared with the native PPase) at different temperatures (\pm SD, $n = 3$).

extension and collapse of pNIPAM chains could fit for the size of the nearby proteins.

From Figure 3, it can be concluded that the introduction of pNIPAM onto the surface of AuNP-PPase can both modulate protein activity drastically (the activity of the conjugates at 45 °C was 270% of that at 25 °C) and realize gradient activity modulation under gradual changes of temperature.

Effect of Molecular Weight of pNIPAM on Activity Modulation of the Conjugates. pNIPAM chains affect the extent of shielding and deshielding of proteins on AuNPs. Below the LCST, pNIPAM should have a molecular weight high enough to offer sufficient blockage of the active sites of PPase, interfering with its approach and its interaction with the substrates. However, the molecular weight of pNIPAM cannot be so high as to dominate the surface while in a dehydrated state above LCST, in which case hydrophobicity-induced AuNP aggregation is expected.²⁵ To realize maximum protein activity modulation of AuNP-PPase-pNIPAM conjugates by temperature change, introducing pNIPAM with an appropriate molecular weight is of great importance. For this purpose, 25 °C (below the LCST) and 45 °C (to ensure the protein activity was not affected by temperature, so we chose 45 °C as the experimental temperature above the LCST) were chosen as contrastive temperatures to study the relative activities of the conjugates with different molecular weights of pNIPAM (Figure 4). When molecular weight of pNIPAM was 5 kDa, the relative activity of the conjugates was approximately 90% at both 25 and 45 °C, showing no obvious difference. When the molecular weight was 10 kDa, the relative activity of the conjugates at 45 °C ($90.3 \pm 3.3\%$) was approximately 200% of that at 25 °C ($49.3 \pm 3.8\%$), showing a significant increase ($P <$

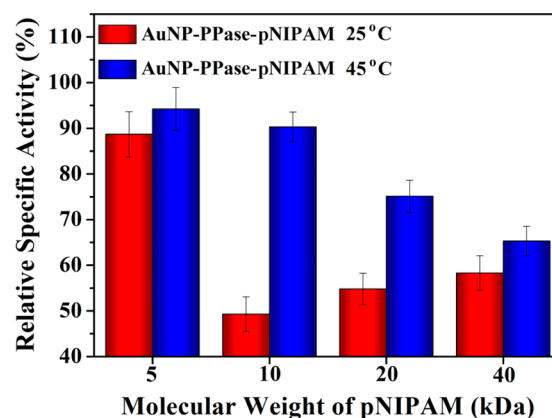


Figure 4. Effect of molecular weight of pNIPAM on activity modulation of the conjugates. Relative specific activity of the conjugates (compared with the native PPase) with different molecular weights of pNIPAM (\pm SD, $n = 3$).

0.001). When pNIPAM was 20 kDa, the relative activity at 45 °C ($75.1 \pm 3.6\%$) increased slightly to approximately 115% of that at 25 °C ($54.8 \pm 2.9\%$). When the molecular weight was even higher, 40 kDa, there was no obvious difference in the relative activity of the conjugates at either 25 °C or at 45 °C (both approximately 60%).

The molecular weight of pNIPAM of 5 kDa was not high enough to offer sufficient blockage of PPase even at temperature below the LCST, so the relative activity of the conjugates showed no distinct changes at different temperatures. When the molecular weight was 10 kDa, below the LCST, the active sites of PPase were sterically shielded by the hydrated pNIPAM chains and prevented from interacting with substrates; above the LCST, pNIPAM chains were collapsed, exposing proteins on AuNPs, leading to the significant recovery of protein activity ($P < 0.001$). However, with higher molecular weights, the effects of steric hindrance on the conjugates were so significant that they interfered with the interaction between PPase and substrates even above the LCST, leading to decreased activity modulation ability.

From these considerations, it may be concluded that when the molecular weight of pNIPAM introduced onto AuNP-PPase was 10 kDa, the conjugates could optimally modulate protein activity depending on the temperature.

Effect of PPase/pNIPAM Molar Ratio on Activity Modulation of the Conjugates. The PPase/pNIPAM molar ratio on the AuNP surface also affects the protein modulation ability of the conjugates at different temperatures. Appropriate pNIPAM coverage could ensure that almost all protein molecules are adequately shielded at temperature below the LCST. The effect of the PPase/pNIPAM molar ratio on AuNPs on the activity modulation of the conjugates was investigated at 25 and 45 °C. The results showed that with the increase of PPase/pNIPAM molar ratio from 0.8/1 to 24.6/1, the relative activity first increased and then gradually decreased, peaking at $184.2 \pm 4.2\%$ when the PPase/pNIPAM molar ratio was 1.4/1 (Figure 5).

When PPase/pNIPAM molar ratio was 0.8/1, the coverage of pNIPAM on AuNPs was higher than that of PPase. Although pNIPAM interfered with the interaction between PPase and substrates below the LCST, high steric hindrance of pNIPAM still affected the recovery of protein activity above the LCST. When PPase/pNIPAM molar ratio rose to 1.4/1, below the

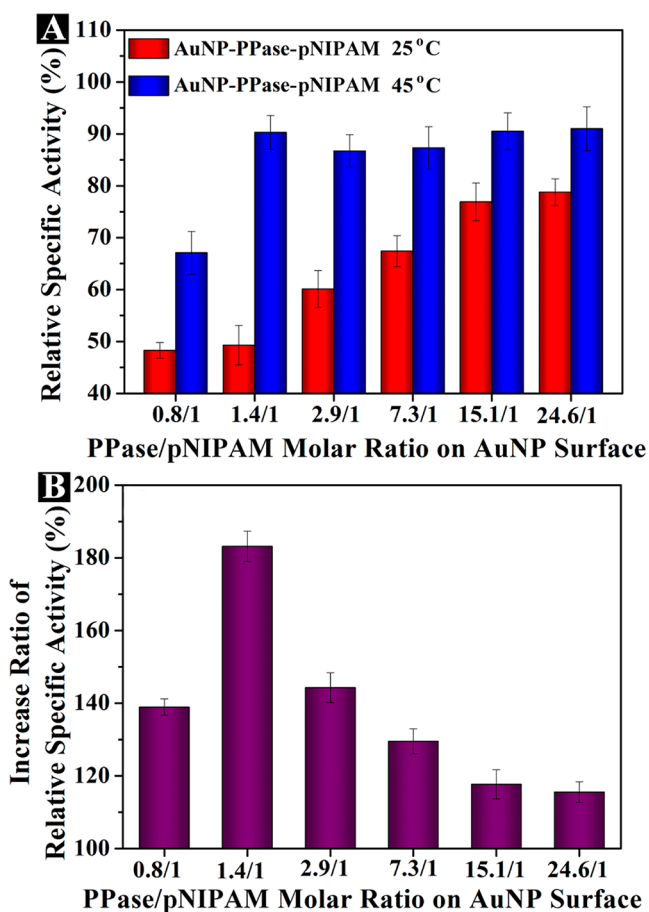


Figure 5. Effect of PPase/pNIPAM molar ratio on activity modulation of the conjugates. (A) Relative specific activity of the conjugates (compared with the native PPase) with different PPase/pNIPAM molar ratios on the AuNP surface (\pm SD, $n = 3$); (B) increased relative specific activity of the conjugates at 45 °C compared with 25 °C with different PPase/pNIPAM molar ratios on the AuNP surface (\pm SD, $n = 3$).

LCST, the hydrated pNIPAM chains sterically shielded the active sites of PPase, affecting the interaction between the active sites and substrates. Above the LCST, pNIPAM chains were collapsed to expose proteins on AuNPs, leading to significant recovery of protein activity ($P < 0.001$). However, with the molar ratio rising even higher, the coverage of PPase on AuNPs was higher than that of pNIPAM. Below the LCST, the shielding effect of pNIPAM on PPase became weaker, leading to the lower increase in the relative specific activity of the conjugates. Therefore, to make pNIPAM shield the proteins well below the LCST and expose them above the LCST, the molar ratio of PPase/pNIPAM should be controlled at around 1.4/1.

Effect of Protein Orientation on Activity Modulation of the Conjugates. The proper orientation of the conjugated protein on the nanoparticle is also very important to modulate the bioactivity of the protein.^{36–38} An inappropriate orientation will adversely affect the interaction of substrates with the active center of proteins. In this experiment, three different conjugates with different protein orientation were achieved through random binding (RB) or orientated binding (OB1 with an introduced thiol near the active center of PPase; OB2 with an introduced thiol far from the active center of PPase), and their activity modulation potentials were studied (Figure 6). For the

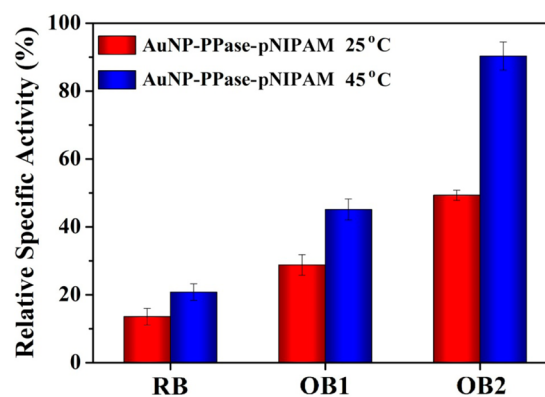


Figure 6. Effect of protein orientation on activity modulation of the conjugates. Relative specific activity of AuNP-RB-pNIPAM, AuNP-OB1-pNIPAM, AuNP-OB2-pNIPAM at 25 and 45 °C (molecular weight of pNIPAM was 10 kDa, PPase: AuNP molar ratio in feed was 100:1) (\pm SD, $n = 3$).

RB, its relative specific activity at 25 °C was very similar to that at 45 °C (approximately 20% different). For the two orientated binding conjugates, their relative activities at 45 °C were both increased compared with those at 25 °C. The increases were approximately 60% for the OB1 and 200% for the OB2, indicating that PPase conjugates with AuNPs via orientated binding, especially for OB2, exhibited significantly increased activity as temperature changed ($P < 0.001$).

From Figure 6, it can be seen that RB (PPase conjugates on AuNPs with random attachment points and no specific orientation) had very low activities and showed a poor modulation of activity with changing temperature. This might be due to the conformational change of the protein, especially the change in active sites caused by random and physical adsorption of PPase on AuNP.^{32,39} For OB1 and OB2, they can bind to AuNP via Au–S bond to give specific site-directed orientations. For OB1, the newly introduced thiol was near the active center (this orientated binding affects the interaction of substrates with the active center of protein), and introducing pNIPAM would more or less influence the conformation of protein active sites and thus the catalytic ability at temperatures below and above the LCST. However, for OB2, on which the introduced thiol is far from the active site (this orientated binding ensures minimal interference with access of substrates and maintains protein activity near the maximum level), when below the LCST, the elongation of pNIPAM chains could well shield the active sites, leading to a low activity ($49.3 \pm 3.8\%$ at 25 °C); when above the LCST, the collapse of pNIPAM chains had minimal interference with the conformation of active center and the access of substrates, leading to a full recovery of activity to $90.3 \pm 3.3\%$ at 45 °C.

On the basis of the data presented, we conclude that when PPase conjugates with AuNPs via random binding, the conjugates cannot modulate protein activity well as temperature changes; when PPase conjugates with AuNPs via orientated binding, the conjugates have apparent potential in modulating protein activity as temperature changes. Particularly, when PPase conjugates with AuNPs at a point far from the active site, the conjugates exhibit a maximum ability for activity modulation by temperature.

Tolerance to Trypsin Digestion of the Native PPase and the Conjugates. In the normal human physiological environment, various and widespread proteases can catalyze the

hydrolysis of peptide bonds, resulting in the conformational changes of proteins or even degradation of proteins.⁴⁰ Thus, enhancing the tolerance to proteases is of great significance for protein–nanoparticle conjugates in biomedical and clinical applications. The tolerance to trypsin digestion of the native PPase and the conjugates was investigated at 25 and 45 °C (Figure 7, tolerance to trypsin digestion at 37 °C see Figure S6

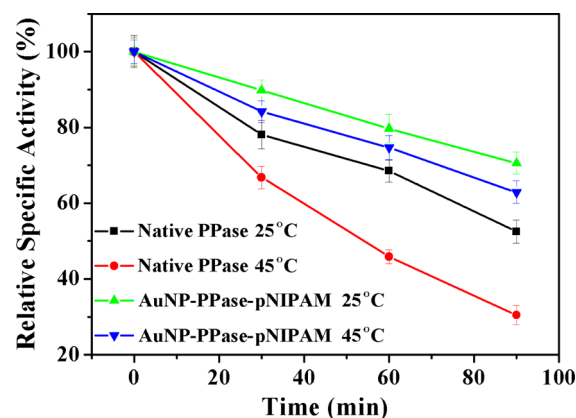


Figure 7. Tolerance to trypsin digestion of the native PPase and the conjugates (\pm SD, $n = 3$).

in the Supporting Information). For both of them, the relative activity decreased gradually with trypsin digestion time, but the degrees of decrease were quite different. After digesting for 90 min, the relative activity at 25 and 45 °C decreased approximately 50 and 70%, respectively, for the native PPase, but only approximately 25 and 30% for the conjugates, demonstrating that AuNP-PPase-pNIPAM conjugates had a much higher resistance to trypsin digestion. This was possibly because the introduction of pNIPAM shielded the protein from trypsin.

4. CONCLUSIONS

In the present work, a new strategy for thermally responsive controllable modulations of protein activity in a protein–nanoparticle conjugate system was established by introducing pNIPAM onto the AuNP-PPase conjugates. The results showed that the activity of the conjugates at 45 °C was approximately 270% of that at 25 °C, and the conjugates exhibited an outstanding ability to modulate protein activity as the temperature changed. This capability of the conjugates was systematically investigated by varying the molecular weight of pNIPAM, the PPase/pNIPAM molar ratio on AuNP, and the orientation of proteins. The conjugates with introduced pNIPAM of 10 kDa, a PPase/pNIPAM molar ratio on AuNPs of 1.4/1, and site-directed orientation with the attachment site far from the active center modulated protein activity the most. The fabrication of AuNP-protein-pNIPAM conjugates can both modulate protein activity drastically and produce a much higher resistance to trypsin digestion, exhibiting great potential in targeted delivery, controllable biocatalysis, and molecular/cellular recognition. Additionally, a wide variety of other stimuli-sensitive materials could readily be incorporated to enable the control of protein inactivation and activation of chemical functionality.

■ ASSOCIATED CONTENT

Supporting Information

The details of the GPC result of ω -COOH pNIPAM, NMR of pNIPAM and pNIPAM-SH, the morphology and size of AuNPs in aqueous solution and AuNP-PPase-pNIPAM, Michaelis–Menten parameters for AuNP-PPase-pNIPAM, immobilized amount of PPase per AuNP, free thiol content of AuNP-PPase-pNIPAM, and the tolerance to trypsin digestion of the conjugates at 37 °C. The Supporting Information is available free of charge on the ACS Publications website at DOI: 10.1021/acsami.5b02502.

■ AUTHOR INFORMATION

Corresponding Authors

*E-mail: wanghw@suda.edu.cn. Tel: +86-512-65880567. Fax: +86-512-65880583.

*E-mail: yuanl@suda.edu.cn

Author Contributions

†F.L. and Y.C. contributed equally. The manuscript was written through contributions of all authors. All authors have given approval to the final version of the manuscript.

Notes

The authors declare no competing financial interest.

■ ACKNOWLEDGMENTS

This work was supported by the National Natural Science Foundation of China (21334004, 21374070, 21474071 and 21474072), National Science Fund for Distinguished Young Scholars (21125418), the Priority Academic Program Development of Jiangsu Higher Education Institutions (PAPD), and the Project of Scientific and Technologic Infrastructure of Suzhou (SZS201207).

■ REFERENCES

- (1) Tsai, D. H.; Delrio, F. W.; Keene, A. M.; Tyner, K. M.; Maccuspie, R. I.; Cho, T. J.; Zachariah, M. R.; Hackley, V. A. Adsorption and Conformation of Serum Albumin Protein on Gold Nanoparticles Investigated Using Dimensional Measurements and In Situ Spectroscopic Methods. *Langmuir* **2011**, *27*, 2464–2477.
- (2) Chen, Y.-S.; Hong, M.-Y.; Huang, G. S. A Protein Transistor Made of An Antibody Molecule and Two Gold Nanoparticles. *Nat. Nanotechnol.* **2012**, *7*, 197–203.
- (3) Ariga, K.; Ji, Q.; Mori, T.; Naito, M.; Yamauchi, Y.; Abe, H.; Hill, J. P. Enzyme Nanoarchitectonics: Organization and Device Application. *Chem. Soc. Rev.* **2013**, *42*, 6322–6345.
- (4) Thompson, A. B.; Calhoun, A. K.; Smagghe, B. J.; Stevens, M. D.; Wotkowicz, M. T.; Hatzioannou, V. M.; Bamdad, C. A Gold Nanoparticle Platform for Protein-Protein Interactions and Drug Discovery. *ACS Appl. Mater. Interfaces* **2011**, *3*, 2979–2987.
- (5) Mahmoud, K. A.; Lam, E.; Hrapovic, S.; Luong, J. H. Preparation of Well-Dispersed Gold/Magnetite Nanoparticles Embedded on Cellulose Nanocrystals for Efficient Immobilization of Papain Enzyme. *ACS Appl. Mater. Interfaces* **2013**, *5*, 4978–4985.
- (6) Zhong, R.; Liu, Y.; Zhang, P.; Liu, J.; Zhao, G.; Zhang, F. Discrete Nanoparticle-BSA Conjugates Manipulated by Hydrophobic Interaction. *ACS Appl. Mater. Interfaces* **2014**, *6*, 19465–19470.
- (7) Sapsford, K. E.; Algar, W. R.; Berti, L.; Gemmill, K. B.; Casey, B. J.; Oh, E.; Stewart, M. H.; Medintz, I. L. Functionalizing Nanoparticles with Biological Molecules: Developing Chemistries that Facilitate Nanotechnology. *Chem. Rev.* **2013**, *113*, 1904–2074.
- (8) Secundo, F. Conformational Changes of Enzymes Upon Immobilisation. *Chem. Soc. Rev.* **2013**, *42*, 6250–6261.
- (9) Shemetov, A. A.; Nabiev, I.; Sukhanova, A. Molecular Interaction of Proteins and Peptides with Nanoparticles. *ACS Nano* **2012**, *6*, 4585–4602.

- (10) Zhou, L.; Chen, Z.; Dong, K.; Yin, M.; Ren, J.; Qu, X. DNA-Mediated Construction of Hollow Upconversion Nanoparticles for Protein Harvesting and Near-Infrared Light Triggered Release. *Adv. Mater.* **2014**, *26*, 2424–2430.
- (11) Song, Y.; Xu, C.; Wei, W.; Ren, J.; Qu, X. Light Regulation of Peroxidase Activity by Spiropyran Functionalized Carbon Nanotubes Used for Label-Free Colorimetric Detection of Lysozyme. *Chem. Commun.* **2011**, *47*, 9083–9085.
- (12) Simons, J. R.; Mosisch, M.; Torda, A. E.; Hilterhaus, L. Site Directed Immobilization of Glucose-6-phosphate Dehydrogenase via Thiol-Disulfide Interchange: Influence on Catalytic Activity of Cysteines Introduced at Different Positions. *J. Biotechnol.* **2013**, *167*, 1–7.
- (13) Jung, Y.; Lee, J. M.; Jung, H.; Chung, B. H. Self-Directed and self-Oriented Immobilization of Antibody by Protein G-DNA Conjugate. *Anal. Chem.* **2007**, *79*, 6534–6541.
- (14) Gagner, J. E.; Lopez, M. D.; Dordick, J. S.; Siegel, R. W. Effect of Gold Nanoparticle Morphology on Adsorbed Protein Structure and Function. *Biomaterials* **2011**, *32*, 7241–7252.
- (15) Wu, X.; Narsimhan, G. Effect of Surface Concentration on Secondary and Tertiary Conformational Changes of Lysozyme Adsorbed on Silica Nanoparticles. *Biochim. Biophys. Acta* **2008**, *1784*, 1694–1701.
- (16) Roach, P.; Farrar, D.; Perry, C. C. Surface Tailoring for Controlled Protein Adsorption: Effect of Topography at the Nanometer Scale and Chemistry. *J. Am. Chem. Soc.* **2006**, *128*, 3939–3945.
- (17) Wu, C. S.; Lee, C. C.; Wu, C. T.; Yang, Y. S.; Ko, F. H. Size-Modulated Catalytic Activity of Enzyme-Nanoparticle Conjugates: a Combined Kinetic and Theoretical Study. *Chem. Commun.* **2011**, *47*, 7446–7448.
- (18) Randolph, L. M.; Chien, M. P.; Gianneschi, N. C. Biological Stimuli and Biomolecules in the Assembly and Manipulation of Nanoscale Polymeric Particles. *Chem. Sci.* **2012**, *3*, 1363–1380.
- (19) Wilson, J. T.; Keller, S.; Manganiello, M. J.; Cheng, C.; Lee, C. C.; Opara, C.; Convertine, A.; Stayton, P. S. pH-Responsive Nanoparticle Vaccines for Dual-Delivery of Antigens and Immunostimulatory Oligonucleotides. *ACS Nano* **2013**, *7*, 3912–3925.
- (20) Yan, Q.; Wang, J.; Yin, Y.; Yuan, J. Breathing Polymersomes: CO₂-Tuning Membrane Permeability for Size-Selective Release, Separation, and Reaction. *Angew. Chem., Int. Ed.* **2013**, *52*, 5070–5073.
- (21) Schild, H. G. Poly (N-Isopropylacrylamide) - Experiment, Theory and Application. *Prog. Polym. Sci.* **1992**, *17*, 163–249.
- (22) Guan, Y.; Zhang, Y. PNIPAM Microgels for Biomedical Applications: From Dispersed Particles to 3D Assemblies. *Soft Matter* **2011**, *7*, 6375–6384.
- (23) Yuan, L.; Wang, H.; Yu, Q.; Wu, Z.; Brash, J. L.; Chen, H. “Nano-catalyst” for DNA Transformation. *J. Mater. Chem.* **2011**, *21*, 6148–6151.
- (24) Wang, H.; Wang, Y.; Yuan, L.; Wang, L.; Yang, W.; Wu, Z.; Li, D.; Chen, H. Thermally Responsive Silicon Nanowire Arrays for Native/Denatured-Protein Separation. *Nanotechnology* **2013**, *24*, 105101.
- (25) Zhang, K.; Zhu, X.; Jia, F.; Auyeung, E.; Mirkin, C. A. Temperature-Activated Nucleic Acid Nanostructures. *J. Am. Chem. Soc.* **2013**, *135*, 14102–14105.
- (26) Mastrotto, F.; Caliceti, P.; Amendola, V.; Bersani, S.; Magnusson, J. P.; Meneghetti, M.; Mantovani, G.; Alexander, C.; Salmaso, S. Polymer Control of Ligand Display on Gold Nanoparticles for Multimodal Switchable Cell Targeting. *Chem. Commun.* **2011**, *47*, 9846–9848.
- (27) Wang, L.; Yuan, L.; Wang, H.; Liu, X.; Li, X.; Chen, H. New Strategy for Reversible Modulation of Protein Activity through Site-Specific Conjugation of Small Molecule and Polymer. *Bioconjugate Chem.* **2014**, *25*, 1252–1260.
- (28) Li, X.; Wang, L.; Chen, G.; Haddleton, D. M.; Chen, H. Visible Light Induced Fast Synthesis of Protein-Polymer Conjugates: Controllable Polymerization and Protein Activity. *Chem. Commun.* **2014**, *50*, 6506–6508.
- (29) Grabar, K. C.; Freeman, R. G.; Hommer, M. B.; Natan, M. J. Preparation and Characterization of Au Colloid Monolayers. *Anal. Chem.* **1995**, *67*, 735–743.
- (30) Heinonen, J. K.; Lahti, R. J. A New and Convenient Colorimetric Determination of Inorganic Orthophosphate and Its Application to the Assay of Inorganic Pyrophosphatase. *Anal. Biochem.* **1981**, *113*, 313–317.
- (31) Bradford, M. M. A Rapid and Sensitive Method for the Quantitation of Microgram Quantities of Protein Utilizing the Principle of Protein-Dye Binding. *Anal. Biochem.* **1976**, *72*, 248–254.
- (32) Liu, F.; Wang, L.; Wang, H.; Yuan, L.; Li, J.; Brash, J. L.; Chen, H. Modulating the Activity of Protein Conjugated to Gold Nanoparticles by Site-Directed Orientation and Surface Density of Bound Protein. *ACS Appl. Mater. Interfaces* **2015**, *7*, 3717–3724.
- (33) Kim, J.-B.; Bruening, M. L.; Baker, G. L. Surface-Initiated Atom Transfer Radical Polymerization on Gold at Ambient Temperature. *J. Am. Chem. Soc.* **2000**, *122*, 7616–7617.
- (34) Lindquist, S. The Heat-Shock Response. *Annu. Rev. Biochem.* **1986**, *55*, 1151–1191.
- (35) Gauthier, M. A.; Klok, H.-A. Polymer–Protein Conjugates: an Enzymatic Activity Perspective. *Polym. Chem.* **2010**, *1*, 1352–1373.
- (36) Kim, H. I.; Hwang, D.; Jeon, S. J.; Lee, S.; Park, J. H.; Yim, D.; Yang, J. K.; Kang, H.; Choo, J.; Lee, Y. S.; Chung, J.; Kim, J. H. Orientation and Density Control of Bispecific Anti-HER2 Antibody on Functionalized Carbon Nanotubes for Amplifying Effective Binding Reactivity to Cancer Cells. *Nanoscale* **2015**, *7*, 6363–6373.
- (37) Mazzucchelli, S.; Colombo, M.; Verderio, P.; Rozek, E.; Andreatta, F.; Galbiati, E.; Tortora, P.; Corsi, F.; Prosperi, D. Orientation-Controlled Conjugation of Haloalkane Dehalogenase Fused Homing Peptides to Multifunctional Nanoparticles for the Specific Recognition of Cancer Cells. *Angew. Chem., Int. Ed.* **2013**, *52*, 3121–3125.
- (38) Colombo, M.; Mazzucchelli, S.; Montenegro, J. M.; Galbiati, E.; Corsi, F.; Parak, W. J.; Prosperi, D. Protein Oriented Ligation on Nanoparticles Exploiting O₆-Alkylguanine-DNA Transferase (SNAP) Genetically Encoded Fusion. *Small* **2012**, *8*, 1492–1497.
- (39) Rusmini, F.; Zhong, Z.; Feijen, J. Protein Immobilization Strategies for Protein Biochips. *Biomacromolecules* **2007**, *8*, 1775–1789.
- (40) Lin, W.; Zhang, H.; Wu, J.; Wang, Z.; Sun, H.; Yuan, J.; Chen, S. A Novel Zwitterionic Copolymer with A Short Poly(Methyl Acrylic Acid) Block for Improving Both Conjugation and Separation Efficiency of A Protein Without Losing its Bioactivity. *J. Mater. Chem. B* **2013**, *1*, 2482–2488.